RESEARCH PAPER

Identification Of Potential HIV Inhibitors Using Virtual Screening and Molecular Modeling Approaches

Kamaldeep Kaur, Piyush Kumar Yadav*, Anish Kumar*

Department of Bioinformatics, School of Bioengineering and Biosciences, Lovely Professional University, Punjab

***Corresponding Author:** *anish.20215@lpu.co.in, kumarpiyush285@gmail.com*

ABSTRACT

Ritonavir is an antiretroviral drug used for the cure of HIV infection. However, according to the medical evidences, the development of an emerged resistance against ritonavir action is due to the occurrence of various mutations in HIV protease gene. It highlights the necessity to develop capable inhibitor for the intervention of ritonavir resistance in HIV protease. In the current research, unique form of lead molecule was recognized using virtual screening, molecular docking and molecular dynamics technique. The virtual screening analysis was performed using PubChem database by applying ritonavir as query and refinement of the data was done via molecular docking approach. The Lipinski rule of five was applied for the investigation of ADMET properties and to evaluate the bioavailability of the compounds. After that, potential drug candidates emerged from screening was tested for the toxicity profiles, drug likeness and other physio-chemical properties of drugs by OSIRIS server. Eventually, to validate the binding property of active compound, molecular dynamics simulation was also implemented. This study evidently confirms that CID:22863038, surely have the potential to inhibit HIV protease undoubtedly effective to tackle the drug resistance in HIV.

Keywords: Drug resistance, Ritonavir, HIV protease, Virtual screening, Molecular docking, Molecular dynamics simulation.

How to cite this article: Kaur K, Yadav P K, Kumar A, Identification Of Potential HIV Inhibitors Using Virtual Screening and Molecular Modeling Approaches. Int J Drug Deliv Technol. 2026;16(6s): 506-528.

Source of support: Nil

Conflict of interest: None

1. INTRODUCTION

A Human Immunodeficiency Virus (HIV) is categorized into two significant types, HIV-1 and HIV-2, with 60% similarity in genetic homology. Nonetheless, the virulence level of HIV-2 is less than HIV-1. Since HIV-1 has been discovered, about 84.2 million infections and 42.3 million deaths were reported worldwide. The World Health Organization (WHO) had put an effort to minimize the HIV-1 infections from 1.5 million to 335,000 and also the death rate from 680,000 to below 240,000 by 2030 at a substantial rate (1). While, antiretroviral therapy (ART) worked out well to tackle the deadly HIV-1 infection by transforming it to attainable long-term condition, still an effective vaccine is required for the satisfactory treatment of HIV (2). India had an approximately >2.5 million individuals suffering with HIV in the 2023 national survey estimates indicating a long-term decline in adult occurrence from the outbreak, nevertheless a notable national significance; the details and district-level numerical data is available in 2023 NACO estimations and factsheets (3). Primarily, adult prevalence was maximum in the late 1990s and early 2000s, and mass prohibition and remedial initiatives in the past twenty years have diminished novel infections and ubiquity in many years(4). However, geographical disproportion still remains obvious: while national prevalence is decreasing, some states such as Maharashtra, Karnataka, Andhra Pradesh, Telangana, and specially the northeastern area still bear excessive load, need state-specific epidemiological research and customized development (5).

HIV is naturally a retrovirus that typically infects CD4+ T cells, macrophages, and dendritic cells. There are different stages of the replication process- viral entry, reverse transcription of RNA into DNA, amalgamation into the host genome, and breakdown of viral polyproteins by HIV protease. (6). These steps are considered as an essential therapeutic target, and no doubt, already available ART procedure comprises nucleoside/nonnucleoside reverse transcriptase inhibitors (NRTIs/NNRTIs), protease inhibitors (PIs), integrase inhibitors, and entry inhibitors. The central most is protease inhibitor specifically Ritonavir in ART regimen (7). In starting, Ritonavir was built as an HIV protease inhibitor, however, these days it is used as pharmacokinetic booster due to its convincing inhibition of cytochrome P450 3A4. There are many side effects

such as hepatoxicity, gastrointestinal effects, metabolic difficulties, and resistance of Ritonavir reported even it was diagnostically effective. One of the major barriers to rational HIV treatment is resistance of Ritonavir drug (8). The drug's affinity gets reduced due to the mutations occur during continuous viral replication in ART pressure. ART procedure is a lifelong therapy which made the disease condition worse, and risk of more side effects like treatment fatigue, and adherence challenges has increased.With these challenges, there is a pressing need of plan that can work to control resistance and make the patient tolerance ability better (9).

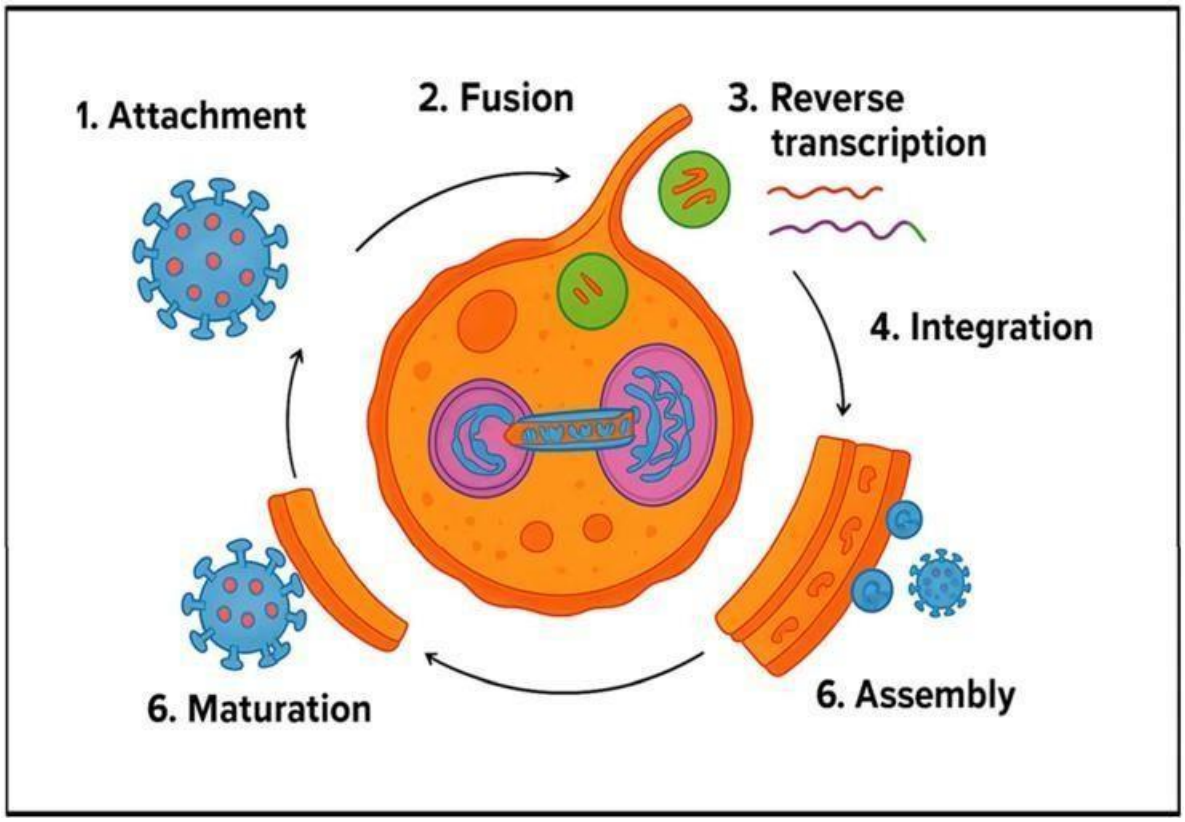

Figure.1. Life cycle of HIV virus (created with smart PPT)- showing key stages including viral attachment, fusion, reverse transcription, integration, assembly, and maturation within the host cell.

Drug repurposing and *Insilico* studies

Drug discovery is a strong approach comes to the true action for speeding up HIV drug discovery. The process includes recognizing novel therapeutic uses for approved drugs or their derivatives, consequently avoiding several early-phase safety assessments (10). The reference drug Ritonavir and related protease inhibitors are potent candidates for derivative repurposing due to their good safety profiles and well-demonstrated pharmacokinetic. It is clear that their antiviral potency can be boosted by just making changes in their structure, also, the toxicity reduction, efficacy restoration can be done against resistant HIV strains (11). Present years have shown that computational methods- from molecular docking and network/knowledge-graph approaches to AI-powered pipelines- can quickly recommend medically helpful repurposed drugs. As an example, expert-amplified in-silico pipeline by BenevolentAI underscored the JAK inhibitor baricitinib as a potent candidate for COVID-19 in early 2020; later biochemical and clinical researches underpinned its anti-inflammatory/antiviral principle and it developed into randomized trials and therapeutic use for acute COVID-19 (12). Standardized investigation of computational repurposing at the time of pandemic shows various in-silico screens manufactured high-affinity compounds that were then proceeded to in-vitro (13), animal, and medical testing, presenting the worth of computational and aligned initiatives used docking and cheminformatics to determine HIV-pointed candidates (for example, in silico screening of protease and polymerase inhibitors that assisted laboratory follow-up), elucidating that these approaches are useful beyond viral disease and therapeutic areas (14).

For repurposing process, computational approaches are playing a key role. For the identification of lead compounds by interactions with HIV targets, techniques such as molecular docking, pharmacophore modeling, molecular dynamics (MD) simulations, and machine learning can quickly screen thousand numbers of compounds in one time

(15). Latest studies established a cultivating role of artificial intelligence (AI) in drug repurposing. As an example, to develop HIV inhibiting molecules with accelerated efficiency in virtual screening, diff4VS originated a diffusion-based generative model influenced by classifiers
(16). Identically, K-Paths raising the level of prediction of drug disease interactions and applications in HIV therapy by implying knowledge-graph reasoning integrate with graph neural-network (GNNs) and large language models (LLMs) (17).
Additionally, improvements are seen in patient identification in electric health records with modern HIV research by clinical informatics (18). In 2025 study, HIV patients are carefully categorized into PrEP, and PEP users schematize to hasten translational pipelines. Promptly by the initiation of computational phenotyping approach, which makes easier to study the drug response in a sorted form. These advancements describe the big role of computational techniques significant to HIV-from developing a drug molecule to real-world applications (19).

Principle of this study

However, In HIV treatment protease inhibitors are playing vital role, the ritonavir derivatives are still in the need of standardized research using advance computational methods. The previous studies were based on the identification of novel inhibitors only; less work has been done on the exploration of optimization of ritonavir scaffold to tackle the resistance or minimizing the side effects (20). Current findings indicates that variants can be formed with upgraded protease binding and outstrip pharmacological properties through structure-based design of ritonavir cognate.
This gap undertaken in current study by implying in silico methods to analyze ritonavir derivatives for potent drug repurposing opposed to HIV protease. We evaluated the impact of change in structure on binding interactions and stability in odds with both wild-type and mutant HIV protease through docking, molecular dynamic simulations, and similarity-based screening. In present research work, focus was on next-generation HIV drug-design and to enlighten the scientific community regarding the role of drug repurposing in escalating antiviral development.

2. MATERIAL AND METHODS

Data collection

The native and mutant three-dimensional (3D) co-ordinates of Ritonavir were obtained from Brookhaven Protein Data Bank (PDB) (https://www.rcsb.org/) for the analysis. The corresponding PDB codes were 4PUO and 7LW6 respectively. The structure was solved with 2.90 Å and 2.38 Å resolutions. Ritonavir was selected as a small molecule for the investigation in this research (21). The SMILE format of the Ritonavir and its derivatives were derived from PubChem (https://pubchem.ncbi.nlm.nih.gov/) and the list of SMILE strings were prepared. The molecular weight and other important factors were taken into account before choosing the SMILE strings for the computational analysis (22).

Virtual Screening

Virtual screening is a technology supported technique used to quickly determine potent phytochemical from vast chemical libraries by anticipating their liability to bind a target molecule. By sorting compounds for experimental analysis, it considerably minimizes the time and cost in early-stage drug discovery (23). In this study, to identify possible inhibitor against HIV, the existing approach called ligand-based virtual screening was applied. To conduct similarity-based screening against compound libraries obtained from PubChem database, a proclaimed inhibitor [Ritonavir] was considered as a query molecule. Lipinski's rule of five was employed to filter out the top hits to check drug-likeness using Swiss ADME (24). Eventually, the chosen compounds were prepared for molecular docking to analyses their binding affinities for both the native (4PUO) and mutant (7LW6) structures of HIV integrase enzyme. Virtual screening is computational tools-based technique in which multistep are performed such as pharmacokinetic profiling, bioactivity prediction, and toxicity analysis using and OSIRIS (25). After the completion of this whole process, the lead molecules with concurring binding profiles, pharmacokinetics, and safety parameters were identified which are capable for future docking and simulation studies (26). ADME (Absorption, Distribution, Metabolism, Excretion) properties and toxicity prediction
Molecular properties of drug candidate such as membrane permeability and bioavailability are analyzed using Lipinski's rule of five. These properties relate to some specific molecular descriptors such as logP (partition coefficient), molecular weight (MW), or counts of hydrogen bond acceptors and donors in a molecule. The "rule of five" were formulated with these properties (27). The rule specifies that molecular weight of molecule should be ≤500, then it can be considered as molecule with good membrane permeability, calculated octanol-water partition coefficient, log P≤5, hydrogen bond donors ≤5, acceptors ≤10 and van der Waals bumps polar surface area (PSA) ≤120 Å2. In the current research, the evaluation of all the molecular properties for all the key compounds were done by using Swiss ADME (http://www.swissadme.ch/). The second most important variable of this study is toxicity prediction which is crucial factor in the analysis of developmental compounds. Indeed, toxicity prediction will finalize the compounds which will pass and ready for further assessment and, failed ones will get rejected (28). In the present work, OSIRIS property explorer program (https://www.organic-chemistry.org/prog/peo/) has been

used to examine the toxicity of lead compounds. There were other factors such as drug likeness and drug score of the lead candidates estimated through OSIRIS. This program does evaluation of the drug likeness of compounds in accordance with the list of about 5300 distinct substructure fragments created by 3300 traded drugs as well as 15,000 publicly available fragments with the corresponding drug likeness. The drug score amalgamates drug-likeliness, cLogP, logS, molecular weight, and toxicity risks. By these factors, we conclude a total value which can be used to estimate the compound's general capability to qualify for a drug (29).

Molecular docking

The process of docking first implicates with defining the binding site of ligand in a receptor protein and after that, dock the ligand into framed site. The data collected from literatures was utilized to analyze the amino acids around the binding site. The key compounds acquired from Swiss ADME server were used in docking analysis (30). To start with, SMILE strings which were used to create three- dimensional structure of all the lead candidates. Eventually, docking algorithm was run with the help of Auto dock Vina server (https://vina.scripps.edu/). The drug molecules were ranked based on the docking score with target protein. For the reference, the geometric score of Ritonavir with the target protein (native and mutant) was considered for refining the lead compounds (31). In this research, rigid receptor-flexible ligand docking analysis was conducted according to working of Auto dock Vina program. The protein file obtained from PDB and energy minimization was done, along with the ligand file submitted as input for the docking (32). The Vina algorithm enlist three bioinformatics tools like Swiss ADME, Molinspiration, fundamental steps for docking- (1) Protein and Ligandpreparation using Auto dock tools (2) Grid formation with target protein (3) Collecting all the files required in one folder as PDB and Pdbqt files of protein and ligand, Vina files, also grid box file as well. (4) Running the command

Molecular dynamics simulation

A computational method known as Molecular Dynamics Simulations is used to examine how protein-ligand complex interactions behave at atomic level. Molecular Dynamics Simulations were conducted using GROMACS Package 2023.3-11.8 with AMBER99SB-ILDN force field and TIP3P water model (33). The complex was packed in cubic periodic box of size 13 × 13 × 13 nm3, verifying a minimum distance of 1.0 nm between the solute and the box edges. Specific water molecules were employed to solvate the system after 9 NA+ ions neutralized it. Steepest descent algorithm was used to perform the energy minimization with a maximum of 5000 steps (34). Under NVT (Canonical Ensemble) and NPT (Isothermal Isobaric Ensemble) circumstances, the system was equilibrated at 300 K and 1.0 bar, categorically, using the V-rescale thermostat (0.1 ps) and the Parrinello-Rahman barostat (2.0 ps) with a 4.5 × 10-5 bar-1 compressive force. To evaluate long-range electrostatics, The Particle Mesh Ewald (PME) method was implemented with cut-off of 10.0 nm for both and filtering the lead compounds on the basis of good geometric score along with the RMSD scores (35). electrostatic and van der Waals interactions. The Leap-frog integrator was applied with a 2-fs time step for a total of 100 ns. The LINCS approach was used to restrict all covalent interactions including hydrogen bonds, establishing numerical stability of the molecular system. The trajectories were examined using XMGRACE tool to calculate RMSD (Root Mean Square Deviation), RMSF (Root Mean Square Fluctuations), SASA (Solvent Accessible Surface Area), Radius of Gyration for analyzing the stability and compactness of the protein ligand complex (36). As you know, RMSD is used to assess the structure stability of a protein-ligand complex throughout molecular dynamics simulations since it calculates the average atomic deviation numerically over time. It constructively demonstrates the fluctuations from its primary conformation. Additional techniques may measure flexibility or compactness, however RMSD promptly exhibit the general stability and convergence of the system (37).

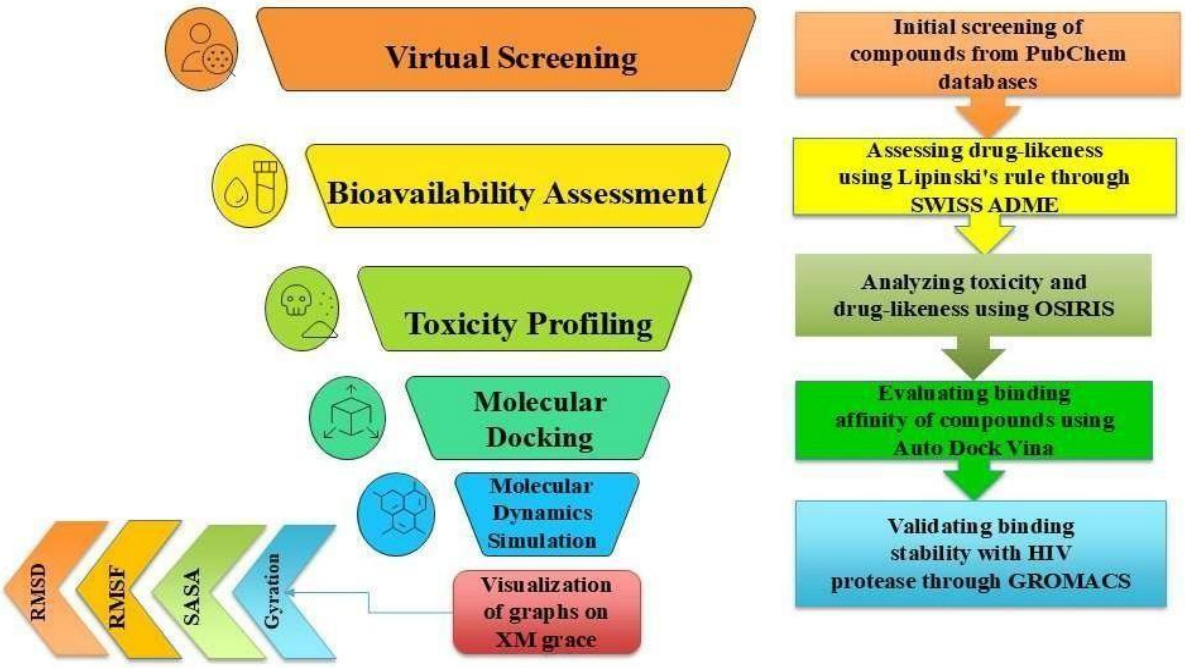

Figure. 2. Overall workflow of the study, including virtual screening, pharmacophore modeling, molecular docking and molecular dynamics simulations, Visualization of graphs via XMgrace for identifying potent HIV inhibitors (created with PowerPoint and Napkin tool)

On the other hand, RMSF is conducted to analyze the flexibility of discrete residues within the protein during the simulation. High mobility regions, such as loops or terminal ends, and stable regions with low fluctuations can be determined with the help of RMSF. The ability to predict the amino acids that are primarily responsible for the dynamic behavior of the protein and its interactions with ligands is thus presented (38). Moreover, Radius of gyration is used to evaluate the tightness and folding stability of the protein structure over the simulation time. A complex with stable Rg value signifies that the protein keeps its structural integrity, whilst higher variations indicate unfolding or conformational changes. Therefore, Rg helps to ensure the overall structural stability of the complex (39). Lastly, SASA investigation evaluates the surface area of the protein attainable to the solvent, bestowing information on protein folding and hydrophobic or hydrophilic disclosure. Variations in SASA during the simulation specifying the conformational rearrangements or ligand binding effects. A stable SASA profile indicates that the protein-ligand complex stayed correctly folded and stable throughout the simulation (40).

3. RESULTS AND DISCUSSION

Virtual screening and bioavailability interpretation

This study started with obtaining the similar structures to ritonavir from the PubChem database. The ritonavir was chosen as the query molecule (41). The correlation cut off was retained up to 99% in the analysis. The total 91 compounds were relinquished. For the further research, these compounds were exploited. SWISS ADME server was used to forecast the bioavailability of ritonavir and the lead candidates. Firstly, the properties of ritonavir were studied through SWISS ADME and managed as control to screen other lead molecules (42). The results are given in Table no.1and 2. It is clear from the table that some of the compounds are violating the rule of five strategy due to difference in molecular weight and increased number of rotatable bonds. This observation does not certainly disqualify the compounds or question their therapeutic relevance. In particular, various approved HIV protease inhibitors, encompassing ritonavir and lopinavir, also contradict the restrained Lipinski rules still keep better clinical potency (43). So, this shows all these compounds may have capability to become the lead drug compound. Nonetheless, toxicity is also one of the vital issues needed to buckle down before choosing the hit compound.

Toxicity analysis

The fundamental point backing the non-success of variety of compounds in drug discovery approach is the problem associated with pharmacokinetics and toxicity. In the current research, OSIRIS property explorer was used to resolve these issues. The variables such as clogP and logS were employed to examine the pharmacokinetic properties of lead compound (44). The result is shown in Table 3. clogP is a fixed value of hydrophilicity of the compound. The increase in logP value may affect the control level due to decreased hydrophilicity of the compound. The value of logP must not be higher than

5.0, for compound to have a rational probability of being fully absorbed. It is clear from the table 3 that logP value of all the 91 compounds established at benchmark.

The attributes of a compound such as absorption and distribution generally get affected by drug solubility. In spite of the fact, compound might be absorbed badly due to inadequate solubility of drug (45). The compound's dissolvability evaluated as log S which is a unit stripped logarithm (base 10) measured in mol/liter. The log S value (forecasted) of more than 80% of the drug which are attainable in the market is more than -4. It is clear from the table 3 that the all the drug molecules are obtained in the equivalent zone with that of specified drugs attaining the acquired solubility.

Drug likeness

The drug likeness is imperious criteria to consider in drug design because compounds retrospect conducive parameters such as absorption, distribution, metabolism, excretion, toxicity (46). The OSIRIS property explorer was practiced to predict the drug-likeness and toxicity profiles of the chosen compounds (47). It was observed that most of the lead compounds showed drug-likeness values more than -10, demonstrate their structural components, which are not well established in present marketed drugs, however still under a considerable range for the lead recognition. These values propose that all the drug molecules might not finely align with standard drug-like fragment patterns, but we cannot firmly disapprove them either.

Drug score and toxicity

Significantly, total 91 compounds were put through toxicity test, and the result signified that 80 compounds were non- tumorigenic, non-mutagenic, and not bound to reproductive or irritant effects. The non-appearance of consequential toxicity problems, in conjunction with approving ADME properties and optimistic docking scores, advices that these compounds hold great potential as hit compounds for advance optimization (48). The compounds such as CID:66832101, CID: 66832099, CID:11350398, CID:66832357, CID:68062464, CID:68973507,CID:69258143 were unsuccessful to pass through the OSIRIS program and exhibit mutagenic and tumorigenic effects. The overall drug score (DS) for all the lead compounds was also evaluated and compared with ritonavir. The result is showed in Table 3. In comparison with standard drug ritonavir, the outlined hits exhibit average to good DS. In current set of data, 3 lead compounds appeared with drug score close to ritonavir. Total 71 compounds selected for further investigation having drug score more than 0.6.

Molecular docking

Molecular docking approach was applied to predict the binding affinity of lead compounds with the target protein. The prediction of active site and grid box setting of native and mutant form of protein was done using BIOVIA and Auto Dock tools based on their 3D structures from PDB database (49). The binding site position of 4PUO was recognized by picking the amino acid residues: LEU100, LYS101, VAL179, TYR181, TYR188, PHE227, TRP229, LEU234, TYR318 and the x, y, z coordinates were calculated to be 28.734, 44.145 and 38.605 and dimensions were set to 40×40×52Å (50). For 7LW6, amino acid residues are: TYR24, HIS41, PHE105, and TYR130, and also the x, y, z, coordinates for mutant form of protein were measured to be 40.470, 15.887, 15.844 and also, grid dimensions were set to 40×40×46Å (51). Docking was performed using 9 binding modes (num_modes = 9) to analyses various possible conformations, and an energy range of 4 k/Cal was implied to obtain poses within a favorable energetic window of the best binding affinity. The docking results are illustrated in Table 4. Both mutant and native forms of protein docked with ritonavir and docking-score of native-type 4PUO-ritonavir complex was -7.5 and for the mutant-type 7LW6-ritonavir, the score was -7.4. The I38T mutant effects the binding of ritonavir with 7LW6 (mutant -type protein) and showed the lesser docking scores. The potent lead compound will be considered as the one with higher docking scores than reference drug molecule, ritonavir. Total 71 lead compounds were docked and out of 41 with unique binding affinity are shown in table. Especially, 16 hit compounds from our data set showed higher docking scores in native- type and with mutant-type and four compounds in mutant-type showed docking scores close to ritonavir. As a case in point, CID:22863038 showed the higher docking scores among the 16 hits in our data repository. The docking score of native-type 4PUO- CID:22863038 complex was determined to be -12.4 kcal/mol and mutant-type 7LW6- CID:22863038 complex was -9.8 kcal/mol. This result demonstrates that CID:22863038 has a good binding affinity with both native and mutant type target protein in comparison with ritonavir.

Molecular dynamics simulation

The atomic level analysis of solvent conditions and stability was performed for the new best hit compound complex with the native and mutant forms of protein. The ligand showed up with convenient binding energy through Molecular Docking approach (52). Molecular Dynamics Simulations were performed at 100 ns for the CID- 22863038 (Hit2) (protein-ligand complex) and compared to CID:59603338 (Hit1), Apo-protein (native and mutant- protein structures without the bound ligand) and also with Ritonavir-protein-complex (control drug and protein (native and mutant) complex).

Both the Apo-protein structures and Hit-2 complex structures showed almost comparable stable conformations up to 100 ns but Hit 1 not, according to the results of RMSD analysis (fig. A and B). The average RMSD values for Hit_2 complex with native protein is 0.34 Å and with mutant protein is 0.22 Å, and value of Hit_1 complex with native is 0.44 Å and mutant is

0.13Å. By comparing these values with the acceptable range 3 Å, the structures are found stable to proceed further for the selection of best hit. The RMSF investigation (fig. C and D) was done for the flexibility check-up of the complexes, which framed the RMS fluctuations of the protein and complex during the 100 ns simulation trajectory. The RMSF figure displayed the loop-like structures that revealed the stability of the Hit_2 complex and Apo protein (Native/Mutant) after~80 ns. At 140 ns, one loop appeared again in both the graphs, but it remained still after. Significantly, positive fluctuations were reported of Hit_2 compared to Hit_1 complex structure. Additionally, the Radius of Gyration (RoG) (fig. E and F) analysis directed that Hit_2 complex was stable after 60 ns. The drop in the curve over 100 ns was seen in the solvent accessible surface area graph specifying the positive result for the selection of Hit_2 as a lead compound (fig. G and H). The similar curves of the RoG and SASA established the validation of the simulation results. Evidently, these results proved the closeness and stability of the protein-ligand complex and approving the authenticity of molecular dynamics simulation.

Table-1-Calculation of molecular properties of lead compound using SWISS ADME

Sr.no.	PubChem CID	MW	TPSA	miLogP	nON	nOHNH	nviolations	Volume
1.	**Ritonavir**	720.94	202.26	5.18	7	4	2	197.82
2.	**CID:**157500168	636.7	182.91	4.04	11	3	1	158.84
3.	**CID:**22858342	525.66	138.02	4.38	6	3	1	143.89
4.	**CID:**22892060	607.76	161.13	4.03	6	4	1	173.35
5.	**CID:**22878494	508.68	145.58	3.39	5	4	1	143.61
6.	**CID:**25097768	511.63	138.02	3.72	6	3	1	139.04
7.	**CID:**25097237	511.63	129.23	4.0	6	2	1	139.18
8.	**CID:**18939520	566.69	179.15	4.03	7	3	1	149.59
9.	**CID:**142994930	599.67	161.13	3.35	9	4	1	154.12
10.	**CID:**18759043	525.66	138.02	4.18	6	3	1	143.89
11.	**CID:**18939781	594.74	179.15	4.7	7	3	1	159.52
12.	**CID:**10218714	599.78	128.79	4.62	5	3	1	171.83
13.	**CID:**130275237	638.7	196.56	3.92	10	4	1	158.09
14.	**CID:**66832101	525.66	149.02	3.26	6	4	1	144.08
15.	**CID:**66832842	576.66	146.38	4.16	7	1	1	163.6
16.	**CID:**171382710	595.75	161.13	4.26	6	4	1	163.08
17.	**CID:**11250237	585.64	161.13	2.93	9	4	1	149.31
18.	**CID:**118875359	620.68	160.88	4.25	10	3	1	155.01
19.	**CID:**46781213	585.83	148.82	4.95	5	4	1	166.28
20.	**CID:**11467322	579.8	148.82	4.9	5	4	1	166.28
21.	**CID:**10196984	627.84	128.79	5.7	5	3	1	181.44
22.	**CID:**168450660	596.74	167.12	4.44	7	4	1	161.27
23.	**CID:**57414227	595.75	161.13	4.65	6	4	1	163.08
24.	**CID:**22863039	561.14	154.81	0.0	6	4	1	152.05
25.	**CID:**22869461	624.79	167.12	3.61	7	4	1	170.93
26.	**CID:**57192617	525.66	138.02	3.97	6	3	1	143.89
27.	**CID:**53959563	524.67	154.81	4.23	6	4	1	145.08
28.	**CID:**124562639	581.73	169.92	3.14	6	5	1	158.18
29.	**CID:**72941970	525.66	138.02	4.51	6	3	1	143.85
30.	**CID:**18758936	525.66	138.02	3.45	6	3	1	143.89
31.	**CID:**66832180	596.74	167.12	3.83	7	4	1	161.01
32.	**CID:**169502032	595.8	169.05	3.93	6	5	1	167.33
33.	**CID:22892061**	607.76	161.13	3.57	6	4	1	173.35
34.	**CID:57404271**	595.75	161.13	3.56	6	4	1	163.08
35.	**CID:60115174**	594.76	157.89	3.88	6	4	1	164.61
36.	**CID:22892062**	593.74	161.13	3.33	6	4	1	168.8

37.	**CID:66832582**	581.73	169.92	2.56	6	5	1	158.18
38.	**CID:10152645**	524.71	108.92	4.78	5	2	1	150.27
39.	**CID:66832099**	525.66	140.23	3.54	6	3	1	144.47
40.	**CID:22863037**	624.79	167.12	4.8	7	4	1	170.93
41.	**CID:456512**	607.76	161.13	3.85	6	4	1	173.61
42.	**CID:71315688**	576.66	146.38	4.08	7	1	1	163.6
43.	**CID:57212162**	566.69	179.15	3.3	7	3	1	149.59
44.	**CID:25096989**	524.67	140.82	3.66	5	4	1	145.61
45.	**CID:56975859**	573.75	161.13	2.95	6	4	1	163.54
46.	**CID:72941971**	550.67	149.1	3.62	6	3	1	156.39
47.	**CID:25096498**	596.74	167.12	3.61	7	4	1	161.01
48.	**CID:456602**	595.75	161.13	3.85	6	4	1	163.08
49.	**CID:22863324**	594.74	179.15	4.29	7	3	1	159.52
50.	**CID:22863038**	524.67	154.81	3.55	6	4	1	145.08
51.	**CID:25096501**	503.63	154.24	2.84	7	3	1	131.91
52.	**CID:25097766**	607.76	161.13	4.02	6	4	1	173.61
53.	**CID:57167325**	410.53	99.69	3.58	4	2	0	115.34
54.	**CID:9845335**	425.54	125.71	2.72	5	3	0	118.05
55.	**CID:18759209**	439.57	125.71	3.08	5	3	0	123.01
56.	**CID:9818282**	313.42	110.77	2.47	4	2	0	83.37
57.	**CID:23367282**	410.53	99.69	3.55	4	2	0	115.34
58.	**CID:11350398**	410.49	137.15	3.0	6	1	0	107.21
59.	**CID:53488159**	462.0	125.71	0.0	5	3	0	125.01
60.	**CID:25096499**	467.58	128.79	2.69	5	3	0	127.96
61.	**CID:10812974**	439.57	125.71	3.08	5	3	0	123.01
62.	**CID:57312003**	439.57	125.71	3.01	5	3	0	122.85
63.	**CID:18759041**	425.54	125.71	3.1	5	3	0	118.05
64.	**CID:10812314**	425.54	125.71	3.25	5	3	0	118.05
65.	**CID:59603312**	377.5	111.72	3.08	5	3	0	103.27
66.	**CID:11101978**	425.54	125.71	2.61	5	3	0	118.05
67.	**CID:53638041**	425.54	125.71	3.69	5	3	0	118.05
68.	**CID:76967449**	369.52	99.77	3.74	4	1	0	102.11
69.	**CID:59603338**	477.62	129.23	4.09	6	2	0	129.11
70.	**CID:71752515**	467.58	128.79	2.77	5	3	0	127.96
71.	**CID:22866454**	439.57	125.71	3.45	5	3	0	123.01
72.	**CID:66832357**	421.51	140.23	2.25	6	3	0	110.33
73.	**CID:66832557**	455.53	152.01	2.38	6	3	0	119.72
74.	**CID:67709217**	483.58	140.23	3.07	6	3	0	130.01
75.	**CID:67748541**	469.55	149.02	2.72	6	4	0	125.11
76.	**CID:67764268**	441.54	145.94	2.82	6	4	0	119.21
77.	**CID:67764269**	496.62	154.81	3.31	6	4	0	135.47
78.	**CID:67764359**	439.57	125.71	3.43	5	3	0	123.01
79.	**CID:67977544**	455.53	152.01	3.04	6	3	0	119.72
80.	**CID:68062464**	477.62	140.23	3.02	6	3	0	129.3
81.	**CID:68972859**	439.57	125.71	3.68	5	3	0	123.01
82.	**CID:68973506**	425.54	125.71	3.1	5	3	0	118.05
83.	**CID:68973507**	421.51	140.23	2.82	6	3	0	110.33
84.	**CID:69256175**	425.54	125.71	2.99	5	3	0	118.05

85.	**CID:69257637**	467.58	120	3.38	5	2	0	128.05
86.	**CID:69257642**	466.64	99.69	4.04	4	2	0	134.31
87.	**CID:69258143**	469.55	149.02	2.25	6	4	0	125.11
88.	**CID:69962921**	440.56	151.73	3.58	6	4	0	120.64
89.	**CID:70019471**	439.57	125.71	3.08	5	3	0	123.01
90.	**CID:70075584**	498.47	125.71	0	5	3	0	131.98
91.	**CID:86621137**	483.58	138.02	3.72	6	3	0	129.43

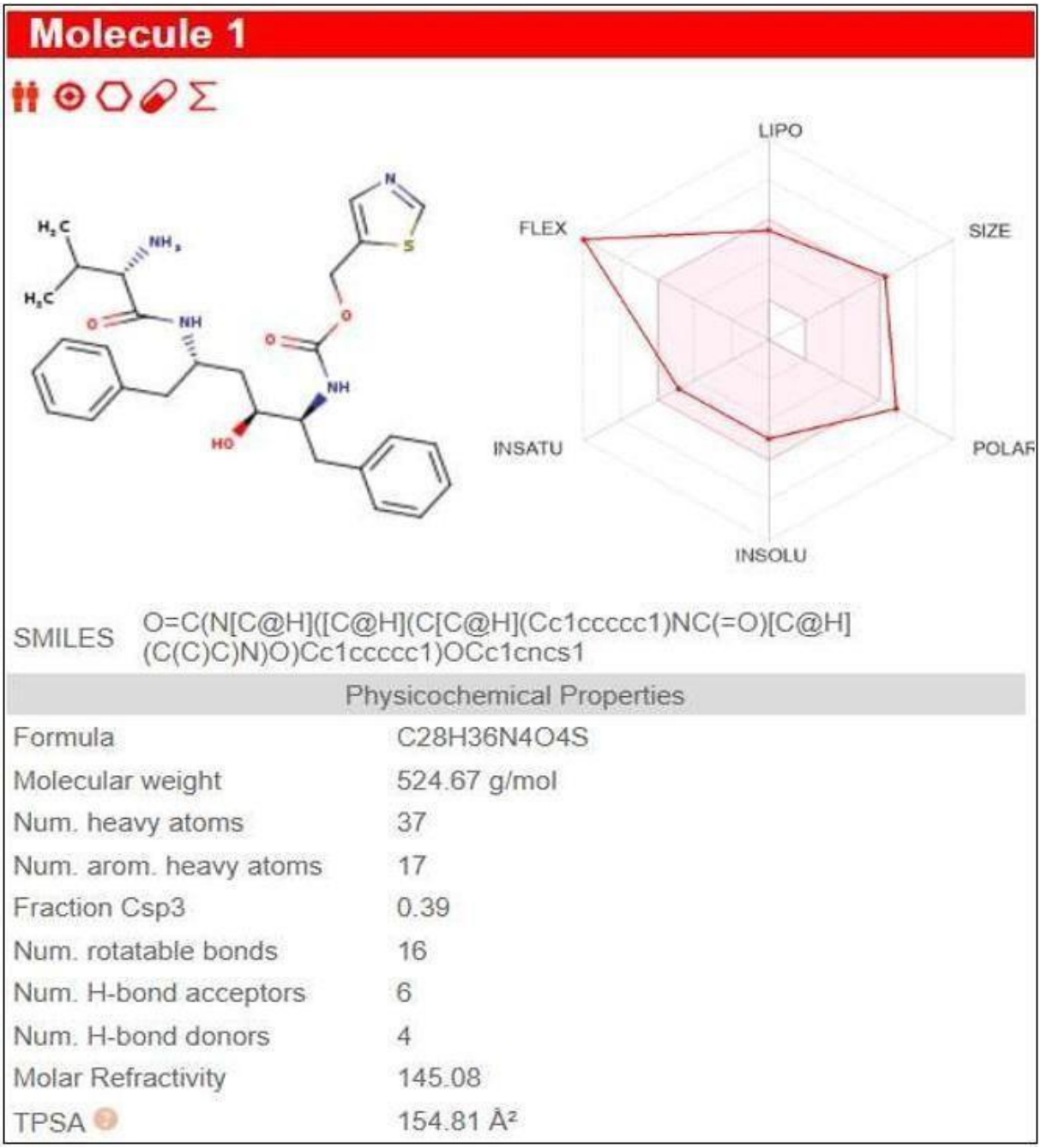

Figure.3: Schematic representation of evaluation of molecular properties of CID-22863038 by using SWISS ADME

Table-2- Details of number of rotatable bonds

Sr.no.	Compound CID	Number of rotatable bonds
1.	**Ritonavir**	22
2.	CID:157500168	17
3.	CID:22858342	16
4.	CID:22892060	17
5.	CID:22878494	15
6.	CID:25097768	16
7.	CID:25097237	15
8.	CID:18939520	17
9.	CID:142994930	17
10.	CID:18759043	16
11.	CID:18939781	17
12.	CID:10218714	18
13.	CID:130275237	17
14.	CID:66832101	15
15.	CID:66832842	12
16.	CID:171382710	19
17.	CID:11250237	16
18.	CID:118875359	19
19.	CID:46781213	17
20.	CID:11467322	17
21.	CID:10196984	19
22.	CID:168450660	20
23.	CID:57414227	20
24.	CID:22863039	16
25.	CID:22869461	20
26.	CID:57192617	16
27.	CID:53959563	16
28.	CID:124562639	19
29.	CID:72941970	17
30.	CID:18758936	16
31.	CID:66832180	19
32.	CID:169502032	17
33.	CID:22892061	17
34.	CID:57404271	20
35.	CID:60115174	19
36.	CID:22892062	17
37.	CID:66832582	19
38.	CID:10152645	15
39.	CID:66832099	15
40.	CID:22863037	20
41.	CID:456512	17
42.	CID:71315688	12
43.	CID:57212162	17
44.	CID:25096989	16
45.	CID:56975859	18
46.	CID:72941971	14
47.	CID:25096498	19
48.	CID:456602	19
49.	CID:22863324	17
50.	CID:22863038	16
51.	CID:25096501	14
52.	CID:25097766	17
53.	CID:57167325	12
54.	CID:9845335	12

55.	CID:18759209	12
56.	CID:9818282	8
57.	CID:23367282	12
58.	CID:11350398	10
59.	CID:53488159	12
60.	CID:25096499	14
61.	CID:10812974	12
62.	CID:57312003	12
63.	CID:18759041	12
64.	CID:10812314	12
65.	CID:59603312	12
66.	CID:11101978	12
67.	CID:53638041	12
68.	CID:76967449	11
69.	CID:59603338	15
70.	CID:71752515	14
71.	CID:22866454	12
72.	CID:66832357	13
73.	CID:66832557	13
74.	CID:67709217	14
75.	CID:67748541	14
76.	CID:67764268	12
77.	CID:67764269	16
78.	CID:67764359	11
79.	CID:67977544	13
80.	CID:68062464	14
81.	CID:68972859	11
82.	CID:68973506	12
83.	CID:68973507	13
84.	CID:69256175	12
85.	CID:69257637	14
86.	CID:69257642	13
87.	CID:69258143	14
88.	CID:69962921	12
89.	CID:70019471	12
90.	CID:70075584	12
91.	CID:86621137	15

Table-3- Tabular representation of toxicity test results obtained from OSIRIS program

Sr.no.	Compound CID	Mutagenic	Tumorigenic	Reproductive effective	cLogP	Solubility	Drug likeness	Drug score
1.	**Ritonavir**	No	No	No	4.72	-6.07	-8.93	0.13
2.	CID:157500168	No	No	No	3.91	-5.28	-19.72	0.22
3.	CID:22858342	No	No	No	4.46	-5.53	-58.62	0.2
4.	CID:22892060	No	No	No	3.85	-5.14	-15.44	0.2
5.	CID:22878494	No	No	No	2.64	-4.3	-1.77	0.34
6.	CID:25097768	No	No	No	4.08	-5.42	-11.7	0.22
7.	CID:25097237	No	No	No	3.89	-4.71	-41.0	0.25
8.	CID:18939520	No	No	No	3.6	-5.17	-13.19	0.22
9.	CID:142994930	No	No	No	3.12	-5.11	-14.23	0.17
10	CID:18759043	No	No	No	4.46	-5.53	-58.62	0.2
11	CID:18939781	No	No	No	4.39	-5.93	-12.61	0.16
12	CID:10218714	No	No	No	6.25	-6.74	-27.83	0.11
13	CID:130275237	No	No	No	2.82	-4.8	-18.04	0.26
14	CID:66832101	Yes	Yes	Yes	4.56	-5.59	-12.86	0.06
15	CID:66832842	No	No	No	4.29	-5.77	1.78	0.33
16	CID:171382710	No	No	No	3.23	-4.82	-11.18	0.22

17	CID:11250237	No	No	Yes	2.66	-4.84	-12.94	0.19
18	CID:118875359	No	No	No	3.79	-5.95	-55.03	0.13
19	CID:46781213	No	No	No	2.85	-4.67	-5.29	0.24
20	CID:11467322	No	No	No	3.83	-5.13	8.47	0.41
21	CID:10196984	No	No	No	6.92	-7.17	-32.36	0.09
22	CID:168450660	No	No	No	3.84	-5.62	-17.72	0.18
23	CID:57414227	No	No	No	3.41	-4.96	-11.46	0.21
24	CID:22863039	No	No	No	2.82	-4.8	-18.04	0.26
25	CID:22869461	No	No	No	4.58	-6.1	-63.72	0.15
26	CID:57192617	No	No	No	4.46	-5.53	-74.84	0.2
27	CID:53959563	No	No	No	2.82	-4.8	-18.04	0.26
28	CID:124562639	No	No	No	2.96	-5.18	-9.36	0.22
29	CID:72941970	No	No	No	4.4	-5.47	-13.23	0.12
30	CID:18758936	No	No	No	4.46	-5.53	-74.84	0.2
31	CID:66832180	No	No	No	4.0	-5.49	-24.96	0.19
32	CID:169502032	No	No	No	2.92	-4.62	7.48	0.47
33	CID:22892061	No	No	No	3.85	-5.14	-15.44	0.2
34	CID:57404271	No	No	No	3.41	-4.96	-11.45	0.21
35	CID:60115174	No	No	No	3.9	-5.43	-10.35	0.19
36	CID:22892062	No	No	No	3.28	-4.96	-7.8	0.22
37	CID:66832582	No	No	No	2.96	-5.18	-9.36	0.22
38	CID:10152645	No	No	No	5.89	-5.64	-57.69	0.16
39	CID:66832099	Yes	Yes	Yes	4.3	-5.04	-12.69	0.11
40	CID:22863037	No	No	No	4.58	-6.1	-63.72	0.15
41	CID:456512	No	No	No	3.62	-5.23	-8.02	0.2
42	CID:71315688	No	No	No	4.29	-5.77	1.78	0.33
43	CID:57212162	No	No	No	3.6	-5.17	-13.19	0.22
44	CID:25096989	No	No	No	3.99	-5.39	-12.78	0.22
45	CID:56975859	No	No	No	3.56	-4.88	-15.62	0.22
46	CID:72941971	No	No	No	3.59	-5.18	-10.02	0.22
47	CID:25096498	No	No	No	4.0	-5.49	-24.96	0.19
48	CID:456602	No	No	No	3.23	-4.82	-11.18	0.22
49	CID:22863324	No	No	No	4.39	-5.93	-12.61	0.16
50	CID:22863038	No	No	No	2.82	-4.8	-18.04	0.26
51	CID:25096501	No	No	No	2.99	-4.9	-11.24	0.27
52	CID:25097766	No	No	No	3.62	-5.23	-8.02	0.2
53	CID:57167325	No	No	No	4.13	-4.55	-13.26	0.3
54	CID:9845335	No	No	No	2.71	-4.23	-13.09	0.34
55	CID:18759209	No	No	No	3.1	-4.61	-11.12	0.31
56	CID:9818282	No	No	No	1.3	-2.1	-5.17	0.46
57	CID:23367282	No	No	No	4.13	-4.55	-17.4	0.3
58	CID:11350398	Yes	Yes	No	0.47	-2.52	-14.1	0.15
59	CID:53488159	No	No	No	2.71	-4.23	-13.09	0.34
60	CID:25096499	No	No	No	3.11	-4.43	-14.04	0.31
61	CID:10812974	No	No	No	3.1	-4.61	-11.12	0.31
62	CID:57312003	No	No	No	2.99	-4.3	-18.74	0.33
63	CID:18759041	No	No	No	2.71	-4.23	-11.68	0.34
64	CID:10812314	No	No	No	2.71	-4.23	-11.68	0.34
65	CID:59603312	No	No	No	1.88	-3.09	-13.0	0.42
66	CID:11101978	No	No	No	2.71	-4.23	-13.09	0.34
67	CID:53638041	No	No	No	2.66	-4.08	-15.64	0.35
68	CID:76967449	No	No	No	2.81	-2.96	5.24	0.49
69	CID:59603338	No	No	No	3.55	-4.11	-46.73	0.3
70	CID:71752515	No	No	No	3.11	-4.43	-14.04	0.31

71	CID:22866454	No	No	No	3.1	-4.61	-12.51	0.31
72	CID:66832357	Yes	Yes	Yes	1.98	-3.2	-4.35	0.12
73	CID:66832557	No	No	No	2.51	-4.55	-12.26	0.32
74	CID:67709217	Yes	Yes	Yes	3.16	-4.25	-11.41	0.16
75	CID:67748541	Yes	Yes	Yes	2.89	-4.61	-12.90	0.09
76	CID:67764268	No	No	No	1.68	-3.83	-12.78	0.36
77	CID:67764269	No	No	No	2.24	-4.26	-17.14	0.31
78	CID:67764359	No	No	No	3.19	-4.62	-6.76	0.31
79	CID:67977544	No	No	No	2.58	-4.54	-9.12	0.32
80	CID:68062464	Yes	Yes	Yes	3.58	-4.18	-9.69	0.09
81	CID:68972859	No	No	No	3.19	-4.62	-8.14	0.31
82	CID:68973506	No	No	No	2.71	-4.23	-11.68	0.34
83	CID:68973507	Yes	Yes	Yes	1.98	-3.2	-4.35	0.12
84	CID:69256175	No	No	No	2.66	-4.08	-15.43	0.35
85	CID:69257637	No	No	No	3.0	-3.87	1.35	0.59
86	CID:69257642	No	No	No	5.79	-5.53	-17.98	0.18
87	CID:69258143	Yes	Yes	Yes	2.89	-4.61	-12.99	0.09
88	CID:69962921	No	No	No	2.08	-3.38	-15.62	0.37
89	CID:70019471	No	No	No	3.1	-4.61	-11.12	0.31
90	CID:70075584	No	No	No	2.71	-4.23	-13.09	0.34
91	CID:86621137	No	No	No	3.32	-4.74	-13.49	0.28

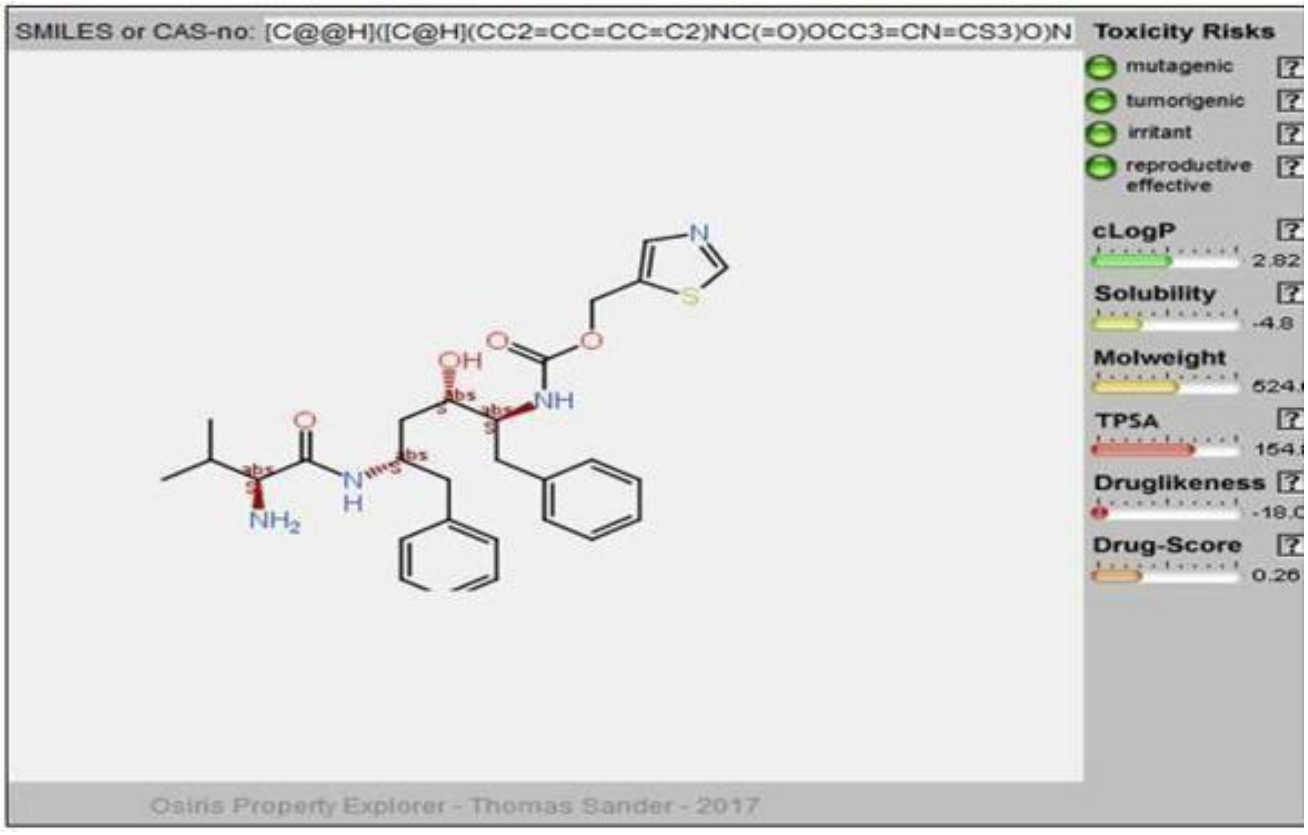

Figure 4: OSIRIS property explorer showing drug likeness properties of CID-22863038

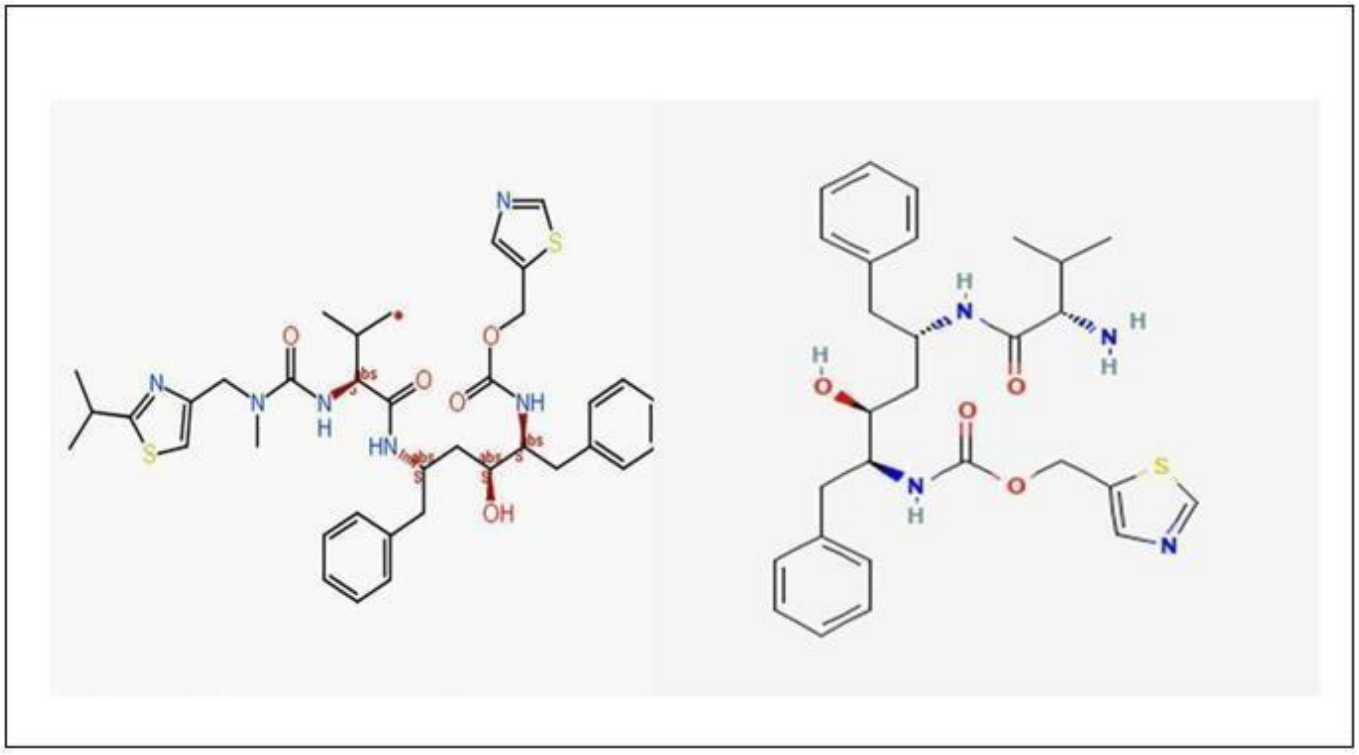

Figure 5: Structure comparison Ritonavir and CID-22863038

Table-4-Tabular representation of lead compounds and native/mutant proteins molecular docking analysis performed with Auto dock Vina

Sr.no.	Compound CID	2D structures	Binding affinity kcal\mol (Native-4PUO)	Mutant (7LW6)
1.	**Ritonavir**	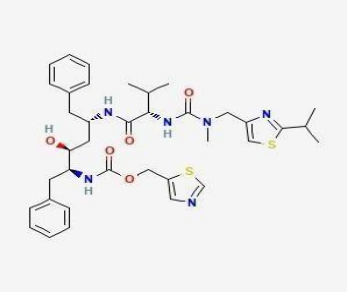	-7.5	-7.4
2.	**CID:22858342**	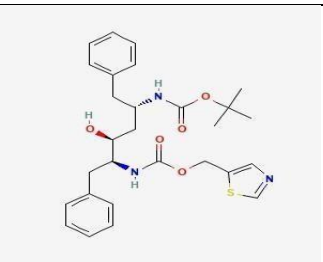	-14.0	-10.5

3.	**CID:118875359**	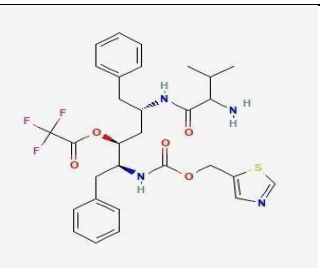	-13.5	-10.0
4.	**CID:25096498**	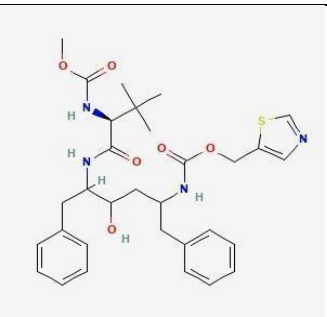	-13.4	-12.4
5.	**CID:56975859**	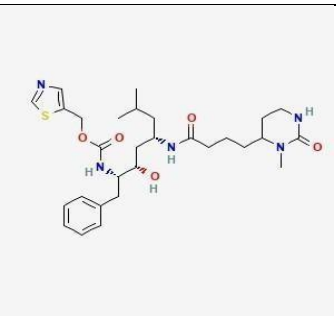	-12.8	-10.0
6.	**CID:57414227**	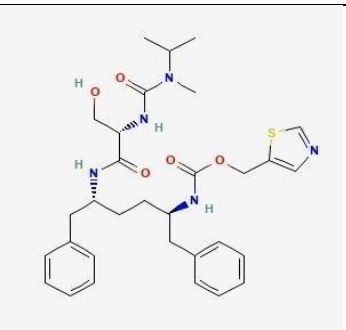	-12.7	-11.4
7.	**CID:59603338**	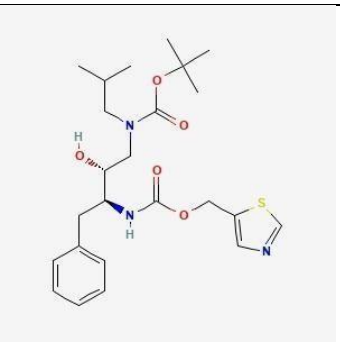	-12.6	-10.2

8.	**CID:18939520**	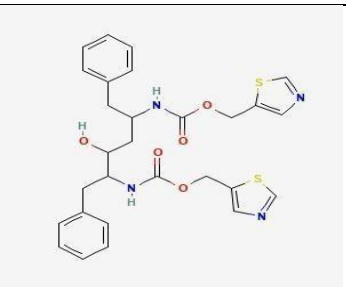	-12.5	-10.9
9.	**CID:22863038**	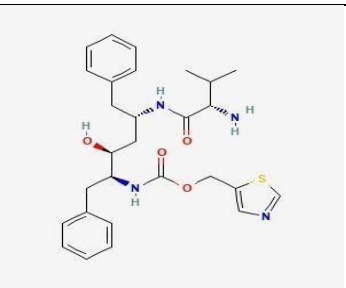	-12.4	-9.8
10.	**CID:57212162**	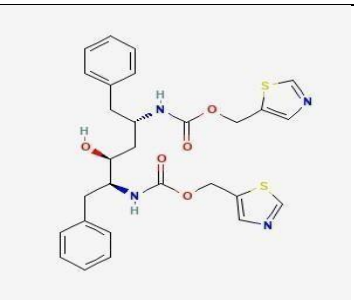	-11.9	-10.3
11.	**CID:71315688**	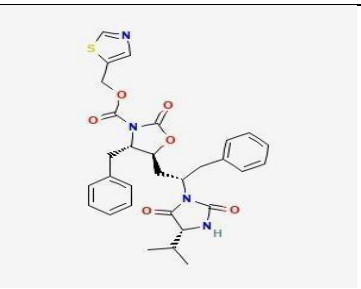	-11.8	-10.9
12.	**CID:22869461**	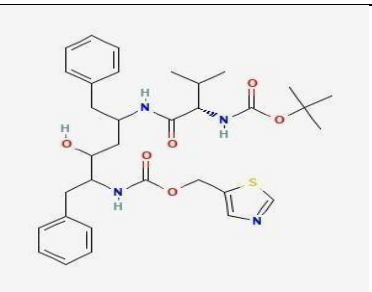	-11.7	-10.1

13.	**CID:456602**	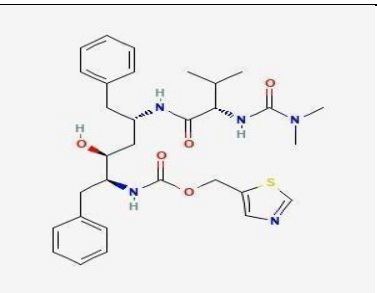	-11.6	-10.7
14.	**CID:171382710**	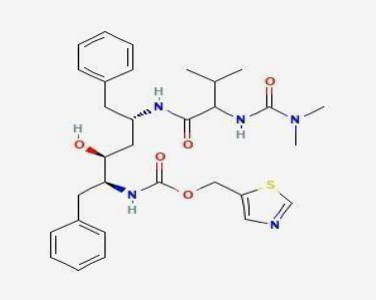	-11.5	-10.7
15.	**CID:22863037**	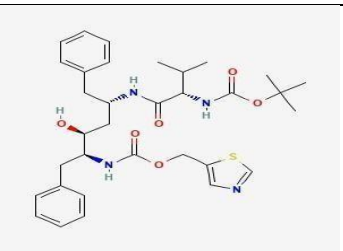	-10.9	-10.1
16.	**CID:168450660**	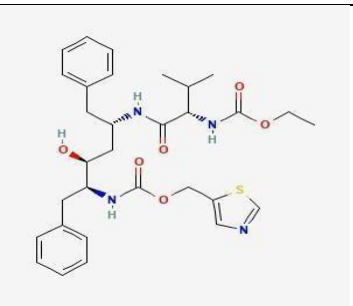	-10.2	-10.0

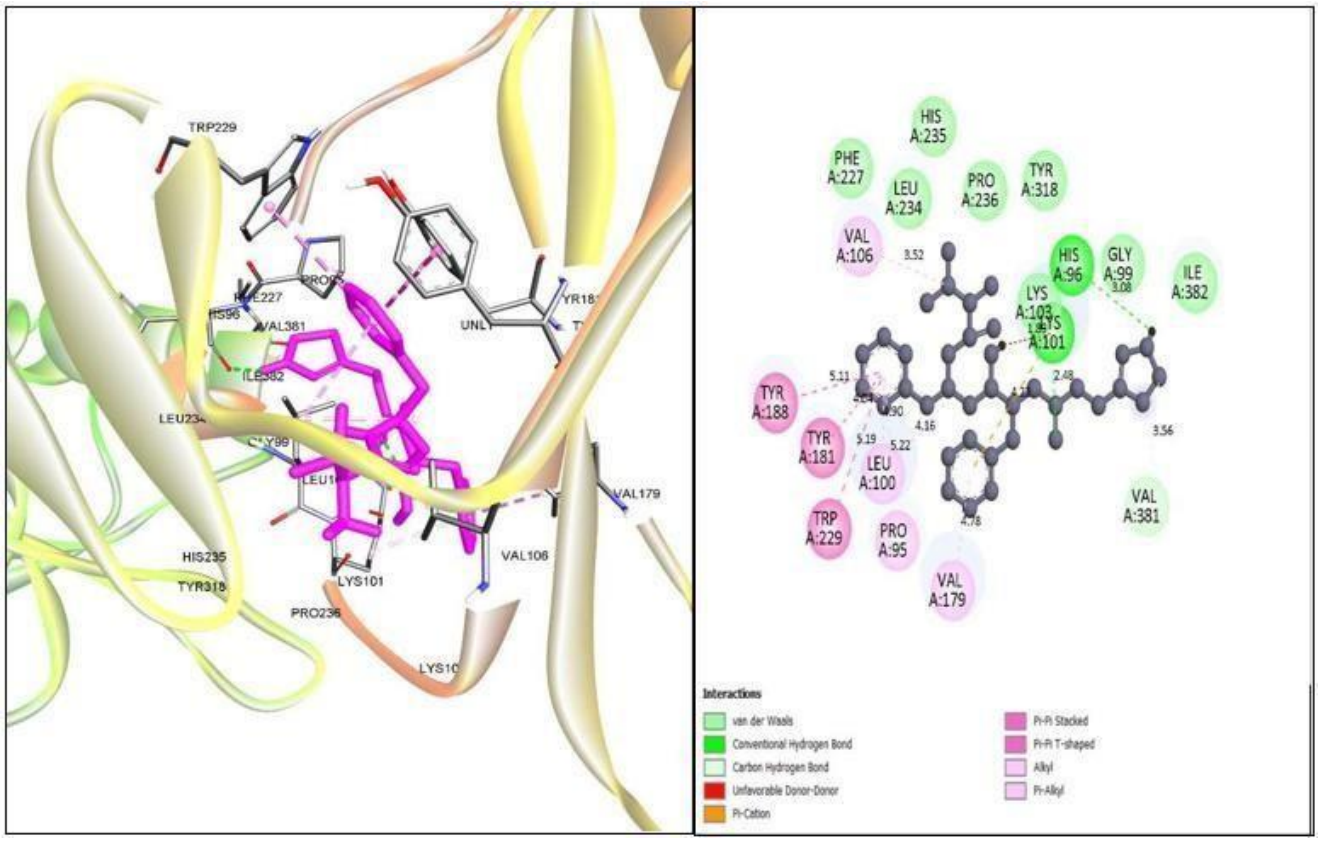

Figure 6: Schematic representation of best-hit compound CID:22863038 complex with native protein 4PUO

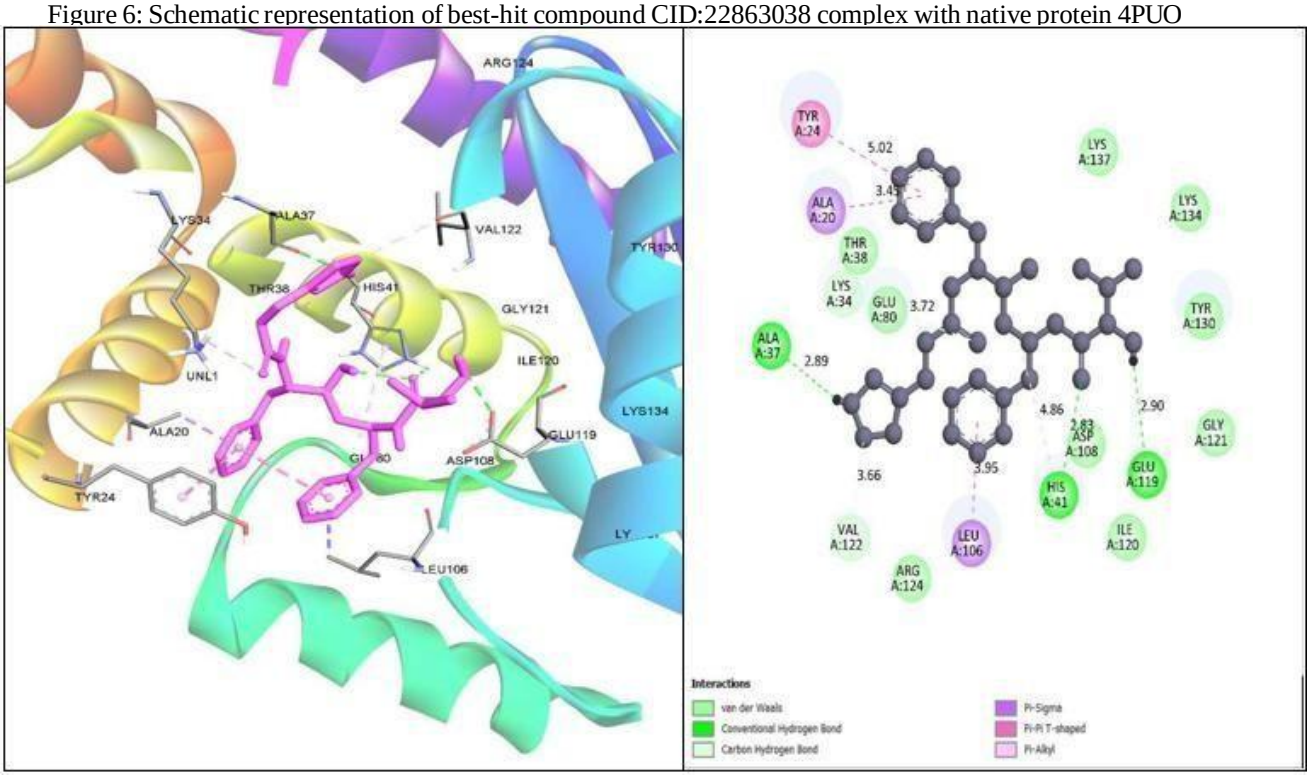

Figure 7: Schematic representation of best-hit compound CID:22863038 complex with mutant protein 7LW6

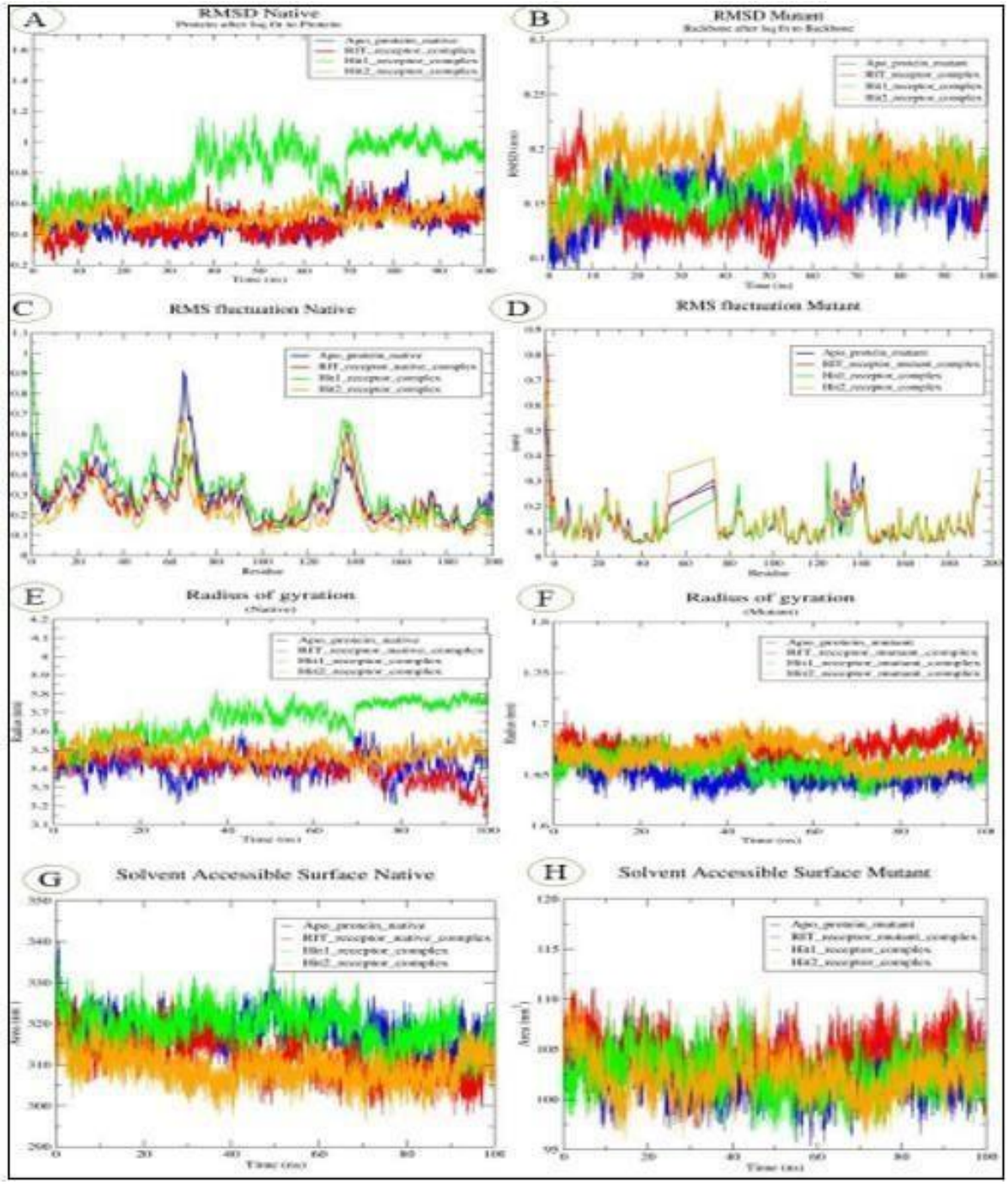

Figure 8: (A) and (B)Root-mean-square-deviation of the Apo-protein-native and Ritonavir control drug, Hit-1 and Hit-2 protein-ligand complexes, (B) and (C) Root-mean-square fluctuation comparison of protein-ligand complexes with control,(D) and (E) Radius of Gyration representing the tightness of protein-ligand complexes, (G) and (H) Solvent Accessible Surface Comparison

4. CONCLUSION

This study revealed possible ritonavir-derived inhibitors that are efficacious against HIV-drug resistant variations utilizing the virtual screening approach. An extensive library of ritonavir analogs was obtained from the PubChem database and analyzed for drug-likeness, pharmacokinetic behavior, and toxicity using SwissADME and OSIRIS Property Explorer. The compounds which passed all the parameter were further exposed to molecular docking analysis using Auto Dock Vina, which disclosed various candidates with strong binding affinities and remarkable interactions with the binding sites of both native and mutant forms of proteins.

This procedure allowed express filtration of thousands of compounds, particularly minimizing the time and cost incorporated with standard experimental screening. Amidst the selected candidates, Hit-1 and Hit-2 exhibited the favorable docking score by interacting with both the proteins. The stability and compactness of best hit were next examined with molecular dynamics simulation approach at 100 ns using GROMACS package 2023.2. CID-22863038 was able to retain the highest level of stability, firmness and favorable interactions when compared to Hit-1 (CID-56975859) and the control (Ritonavir), corresponding to the analysis of RMSD, RMSF, SASA and radius of gyration trajectories. Overall, these findings underscore CID-22863038 as a promising lead molecule with potential effectiveness against HIV drug resistance. The discoveries from this phase entrenched a robust foundation for succeeding computational validation, including pharmacophore modeling and molecular dynamics simulations. Moreover, our research correlates with experimental findings.

REFERENCES

1. Fang Z, Jiang W, Liu P, Xia N, Li S, Gu Y. Targeting HIV-1 immune escape mechanisms: Key advances and challenges in HIV-1 vaccine design. Microbiol Res [https://doi.org/10.1016/j.micres.2025.128229]. 2025;299:128229.
2. Liao Y, Wen Z, Shi M, Zou H, Sun C. Biomedical Interventions for HIV Prevention and Control: Beyond Vaccination. Viruses [https://doi.org/10.3390/v17060756]. 2025;17(6).
3. Kumar P, Das C, Deo V, Chaturvedi HK, Biswas S, Priyam N, et al. Progress and challenges towards eliminating vertical transmission of HIV in India. Sci Rep. 2025;15(1):25004. Available from: https://doi.org/10.1038/s41598-025-09481-2
4. Sahu D, Kumar P, Chandra N, Rajan S, Shukla DK, Venkatesh S, et al. Findings from the 2017 HIV estimation round & trend analysis of key indicators 2010-2017: Evidence for prioritizing HIV/AIDS programme in India. Indian Journal of Medical Research. 2020;151(6). doi: 10.4103/ijmr.IJMR_1619_19
5. Jadhav S, Nair A, Mahajan P, Nema V. The Crosstalk Between HIV-TB Co-Infection and Associated Resistance in the Indian Population. Venereology. 2024;3(4):183–98. Available from:https://doi.org/10.3390/venereology3040015 Available from: https://doi.org/10.1002/eji.200737441
6. Labarile M, Schoepf IC, Pasin C, Oumelloul MA, Thorball CW, Riebensahm C, et al. Untargeted Metabolite Profile Associations with Body Mass Index, Waist-Hip Ratio, and Antiretroviral Therapy in >1300 People with HIV: the Swiss HIV Cohort Study. J Infect Dis. 2025 Aug 27;jiaf438. Available from: https://doi.org/10.1093/infdis/jiaf438
7. He J, Liu J, Song A. "It's time … to end everything": Discontinue medication choices and narratives among elderly HIV-positive Yi women. Soc Sci Med. 2025;383:118450. Available from: https://doi.org/10.1016/j.socscimed.2025.118450
8. Theivendren P, Narayanasamy P, Chidamabaram K, Menon S, Dhivya Antony Sahayaraj JA, Kiruthiga N, et al. In-depth review of breast cancer and inflammation pre-and post-treatment strategies with conventional and novel Steroid agents. Adv Biol Regul. 2025;97:101102. Available from:https://doi.org/10.1016/j.jbior.2025.101102
9. Abdullahi T, Gemou I, Nayak N V, Murtaza G, Bach SH, Eickhoff C, et al. K-Paths: Reasoning over Graph Paths for Drug Repurposing and Drug Interaction Prediction. In: Proceedings of the 31st ACM SIGKDD Conference on Knowledge Discovery and Data Mining V2. New York, NY, USA: Association for Computing Machinery; 2025. p. 5–16. (KDD '25). Available from: https://doi.org/10.1145/3711896.3737011
10. Clavel F, Hance AJ. HIV Drug Resistance. New England Journal of Medicine. 2004;350(10):1023–35. Available from: https://www.nejm.org/doi/full/10.1056/NEJMra025195
11. Smith DP, Oechsle O, Rawling MJ, Savory E, Lacoste AMB, Richardson PJ. Expert-Augmented Computational Drug Repurposing Identified Baricitinib as a Treatment for COVID-19. Front Pharmacol. 2021;Volume 12-2021. Available from: doi: 10.3389/fphar.2021.709856
12. Mohamed K, Yazdanpanah N, Saghazadeh A, Rezaei N. Computational drug discovery and repurposing for the treatment of COVID-19: A systematic review. Bioorg Chem. 2021;106:104490. Available from: https://doi.org/10.1016/j.bioorg.2020.104490
13. Devaraji M, Ravikumar L. In Silico Evaluation of HIV Protease and RNA Polymerase Inhibitors as Potential COVID-19 Therapeutics. Cureus. 2024 Sep;16(9):e69576. Available from: doi:10.7759/cureus.69576
14. Kitchen DB, Decornez H, Furr JR, Bajorath J. Docking and scoring in virtual screening for drug discovery: methods and applications. Nat Rev Drug Discov. 2004;3(11):935–49. Available from:https://doi.org/10.1038/nrd1549
15. Lyu J, Chen C, Liang B, Zhang Y. Diff4VS: HIV-inhibiting Molecules Generation with Classifier Guidance Diffusion for Virtual Screening. In: 2024 IEEE International Conference on Bioinformatics and Biomedicine (BIBM). 2024. p. 721–6. DOI:10.1109/BIBM62325.2024.10822129

16. Sever B, Otsuka M, Fujita M, Ciftci H. A Review of Warner C. Greene. A history of AIDS: looking back to see ahead. Cold Spring Harb Perspect Med. 2011;1(1):a006882.
17. FDA-Approved Anti-HIV-1 Drugs, Anti-Gag Compounds, and Potential Strategies for HIV-1 Eradication. Int J Mol Sci. 2024;25(7):3659. Available from: https://doi.org/10.3390/ijms25073659
18. Haldar A, Yadav KK, Singh S, Yadav PK, Singh AK. In silico analysis highlighting the prevalence of BCL2L1 gene and its correlation to miRNA in human coronavirus (HCoV) genetic makeup. Infection, Genetics and Evolution. 2022;99:105260. Available from: https://doi.org/10.1016/j.meegid.2022.105260
19. Oyediran KO, Bassey POO, Ogundemuren DA, Abdulraheem A, Azubuike CP, Amenaghawon AN, et al. Artificial intelligence in human immunodeficiency virus mutation prediction and drug design: Advancing personalized treatment and prevention. Pharmaceutical Science Advances. 2025;3:100080. Available from: https://doi.org/10.1016/j.pscia.2025.100080
20. de Souza MM, Gini ALR, Moura JA, Scarim CB, Chin CM, dos Santos JL. Prodrug Approach as a Strategy to Enhance Drug Permeability. Pharmaceuticals [Internet]. 2025;18(3). Available from: https://doi.org/10.3390/ph18030297
21. Ye PP, Yao BF, Yang Y, Yang XM, Li Q, Song LL, et al. Drug-drug interactions of simnotrelvir/ritonavir: an open-label, fixed-sequence, two-period clinical trial. Clinical Microbiology and Infection. 2025;31(1):101–7. Available from: DOI:10.1016/j.cmi.2024.09.007
22. Kumar A, Shanthi V, Ramanathan K. Discovery of potential ALK inhibitors by virtual screening approach. 3 Biotech. 2016;6(1):21. Available from: https://doi.org/10.1007/s13205-015-0336-z
23. Gangwal A, Lavecchia A. Artificial intelligence in preclinical research: enhancing digital twins and organ-on- chip to reduce animal testing. Drug Discov Today. 2025;30(5):104360. Available from: https://doi.org/10.1016/j.drudis.2025.104360
24. Bhatkhande Karishma and Vysyaraju NN and ARR and GKM. Recent Advances in Drug-Likeness Screening by Using the Software and Online Tools. In: Rao G. S.N. Koteswara and Alavala RR, editor. Applications of Computational Tools in Drug Design and Development. Singapore: Springer Nature Singapore; 2025. p. 683–717. Available from: https://doi.org/10.1007/978-981-96-4154-3_19
25. Ahsan R, Paul S, Alam MS, Rahman AFMM. Synthesis, Biological Properties, In Silico ADME, Molecular Docking Studies, and FMO Analysis of Chalcone Derivatives as Promising Antioxidant and Antimicrobial Agents. ACS Omega. 2025 Feb 11;10(5):4367–87. Available from: https://doi.org/10.1021/acsomega.4c06897
26. Karthick V, Ramanathan K, Shanthi V, Rajasekaran R. Identification of Potential Inhibitors of H5N1 Influenza A Virus Neuraminidase by Ligand-Based Virtual Screening Approach. Cell Biochem Biophys. 2013;66(3):657–69. Available from: https://doi.org/10.1007/s12013-012-9510- 7
27. Kharatyan L, Gevorgyan S, Khachatryan H, Shavina A, Hakobyan A, Matevosyan M, et al. Data-driven discovery of chemical signatures for developing new inhibitors against human influenza viruses. BMC Chem. 2025;19(1):159. Available from: https://doi.org/10.1186/s13065-025-01540-z
28. Varini C, Manganelli M, Scardala S, Antonelli P, Losasso C, Testai E. An Update of Tetrodotoxins Toxicity and Risk Assessment Associated to Contaminated Seafood Consumption in Europe: A Systematic Review. Toxins (Basel). 2025;17(2). Available from: https://doi.org/10.3390/toxins17020076
29. Cross C, Martinez MN, Pade D, Myers MJ, Neuhoff S. A Bottom-up Approach for Mutant and Wild Type Collies Using Physiologically Based Pharmacokinetic (PBPK) Modeling: A Case Study Using Loperamide. AAPS J. 2025;27(4):101. Available from: https://doi.org/10.1208/s12248-025-01061-6
30. Riaz R, Parveen S, Shafiq N, Ali A, Rashid M. Virtual screening, ADME prediction, drug-likeness, and molecular docking analysis of Fagonia indica chemical constituents against antidiabetic targets. Mol Divers . 2025;29(2):1139– Available from: https://doi.org/10.1007/s11030-024- 10897-7
31. Sen S, Dutta K, Borthakur MS, Chetia D, Tayeng D, Zothantluanga JH, et al. Comparative in-silico study on the antimalarial, anti-HIV, and diuretic properties of a series of substituted bis-2-hydroxy-1,4-naphthoquinone derivatives. Discover Chemistry. 2025;2(1):46. Available from: https://doi.org/10.1007/s44371-025-00114-1
32. Varghese A, Liu J, Patterson TA, Hong H. Integrating Molecular Dynamics, Molecular Docking, and Machine Learning for Predicting SARS-CoV-2 Papain-like Protease Binders. Molecules. 2025;30(14). Available from: https://www.mdpi.com/1420-3049/30/14/2985
33. Alanazi A, Younas S, Khan MU, Saleem H, Alruwaili M, Abdalla AE, et al. A combined in silico and MD simulation approach to discover novel LpxC inhibitors targeting multiple drug resistant

Pseudomonas aeruginosa. Sci Rep. 2025;15(1):16900. Available from: https://doi.org/10.1038/s41598-025-99215-1

34. Grewal S, Deswal G, Grewal AS, Guarve K. Chapter Eight - Molecular dynamics simulations: Insights into protein and protein ligand interactions. In: Narayan CV, Verma S, Grewal AS, Singh N, Nimesh H, editors. Advances in Pharmacology. Academic Press; 2025. p. 139–62. Available from: DOI:10.1016/bs.apha.2025.01.007
35. Yadav PK, Ojha KK, Kumar A, Singh AK. 3D-QSAR based computational screening of potent ligands against L- type calcium channel (LTCC) protein structure for iron overload in β-thalassemia. Comput Biol Med. 2025;194:110551. Available from: https://doi.org/10.1016/j.compbiomed.2025.110551
36. Khamto N, Boontawee P, Choommongkol V, Pruksaphon K, Patnin S, Suree N, et al. Discovery of Galloyl–Flavonoid Conjugates as SARS-CoV-2 3CLpro Inhibitors: Understanding Binding Interactions Through Computational Approaches. Int J Mol Sci .2025;26(19). Available from: https://doi.org/10.3390/ijms26199742
37. Klewicki J, Sandberg R, Knopp T, Devenport W, Fritsch D, Vishwanathan V, et al. On the physical structure, modelling and computation-based prediction of two-dimensional, smooth-wall turbulent boundary layers subjected to streamwise pressure gradients. Journal of Turbulence. 2024 Nov 1;25(10–11):345–68. Available from: https://doi.org/10.1080/14685248.2024.2392572
38. Rubina, Moin ST, Haider S. Identification of a Cryptic Pocket in Methionine Aminopeptidase-II Using Adaptive Bandit Molecular Dynamics Simulations and Markov State Models. ACS Omega. 2024 Jul 2;9(26):28534–45. Available from: https://doi.org/10.1021/acsomega.4c02516
39. Sahoo S, Gosu V, Lee HK, Shin D. Deciphering the conformational changes induced by high-risk nsSNPs in β-lactoglobulin. Heliyon. 2024 Nov 15;10(21). Available from https://doi.org/10.1016/j.heliyon.2024.e40040
40. Ganesh B, Banerjee A, Guruprasad L. Evaluating the ability of in silico identified hit compounds to bind Staphylococcus aureus LcpASA using steered molecular dynamics simulations. Mol Divers. 2025; Available from: https://doi.org/10.1007/s11030-025-11155-0
41. Kumar D, Karuppasamy R. Exploring the structural and functional impact of the ALK F1174L mutation using bioinformatics approach. J Mol Model. 2014 Jul 1;20:2324. DOI: 10.1007/s00894-014-2324-3
42. Lenda F, Er-Rajy M, El Cadi A, Imtara H, Guenoun F, Allouchi H, et al. Molecular docking, dynamic molecular simulation and in silico ADMET screening study of novel bidentate tetrazolyl-adipate anti- HIV drugs candidate. Chinese Journal of Analytical Chemistry.2025;53(3):100498. Available from: https://doi.org/10.1016/j.cjac.2025.100498
43. Okafor SN, Angsantikul P, Ahmed H. Discovery of Novel HIV Protease Inhibitors Using Modern Computational Techniques. Int J Mol Sci. 2022;23(20). Available from: https://doi.org/10.3390/ijms232012149
44. Kumar D, Karuppasamy R. Analyzing resistance pattern of non-small cell lung cancer to crizotinib using molecular dynamic approaches. Indian J Biochem Biophys. 2015 Feb 1;52:23–8.
45. Lipinski CA, Lombardo F, Dominy BW, Feeney PJ. Experimental and computational approaches to estimate solubility and permeability in drug discovery and development settings. Adv Drug Deliv Rev. 1997;23(1):3– Available from: https://doi.org/10.1016/S0169- 409X(96)00423-1
46. Elshobary ME, Badawy NK, Ashraf Y, Zatioun AA, Masriya HH, Ammar MM, et al. Combating Antibiotic Resistance: Mechanisms, Multidrug-Resistant Pathogens, and Novel Therapeutic Approaches: An Updated Review. Pharmaceuticals. 2025;18(3). Available from: https://doi.org/10.3390/ph18030402
47. Rapuru R, Begum RF, Singh SA, Vellapandian C, Ali N, AlAsmari AF, et al. Exploring the therapeutic potential of leriodenine and nuciferine from Nelumbo nucifera for renal fibrosis: an In-silico analysis. 2025; Available from: https://doi.org/10.1515/znc-2024-0229
48. Kumar D. Open source software tools for computer aided drug design. International Journal of Research in Pharmaceutisscal Sciences. 2018 Mar 12;9. DOI:10.26452/IJRPS.V9I1.1191
49. Singh S, Yadav PK, Singh AK. Structure based High- Choudhary S, Khan NS, Saxena P, Sahu P, Pradhan D, Singh H, et al. Repurposing FDA approved drugs for psoriasis indications through integrated molecular docking, one-SVM algorithm, and molecular dynamics simulation approaches. Sci Rep. 2025;15(1):21211. Available from: https://doi.org/10.1038/s41598-025-01448-7

50. Dosunmu DP, Abolade RO, Bashiru M, John-Joy Owolade A, Samuel MK, Boluwatife EO, et al. In silico identification of potential HDAC3 inhibitors through machine learning, molecular docking, and molecular dynamics simulations for drug repurposing. Aspects of Molecular Medicine. 2025;6:100092. Available from: https://doi.org/10.1016/j.amolm.2025.100092
51. Yadav PK, Singh S, Singh AK. '3D-QSAR-based, pharmacophore modelling, virtual screening, and molecular docking studies for identification of hypoxia- inducible factor-1 inhibitor with potential bioactivity. Comput Biol Med. 2023;166:107557. Available from: https://doi.org/10.1016/j.compbiomed.2023.107557
52. Throughput virtual screening, molecular docking and molecular dynamics study of anticancer natural compounds against fimbriae (FimA) protein of Porphyromonas gingivalis in oral squamous cell carcinoma. Mol Divers. 2024;28(3):1141–1152. Available from: https://doi.org/10.1007/s11030-023-10634-6